

## Grazing incidence neutron spin echo spectroscopy: instrumentation aspects and scientific opportunities

This content has been downloaded from IOPscience. Please scroll down to see the full text.

2014 J. Phys.: Conf. Ser. 528 012025

(<http://iopscience.iop.org/1742-6596/528/1/012025>)

View [the table of contents for this issue](#), or go to the [journal homepage](#) for more

### Download details:

IP Address: 134.94.122.242

This content was downloaded on 29/07/2014 at 09:59

Please note that [terms and conditions apply](#).

# Grazing Incidence Neutron Spin Echo Spectroscopy: Instrumentation Aspects and Scientific Opportunities

O. Holderer<sup>1</sup>, H. Frielinghaus<sup>1</sup>, S. Wellert<sup>2</sup>, F. Lipfert<sup>1</sup>, M. Monkenbusch<sup>3</sup>, R. von Klitzing<sup>2</sup>, D. Richter<sup>1,3</sup>

<sup>1</sup>Jülich Centre for Neutron Science (JCNS) at Heinz Maier-Leibnitz Zentrum (MLZ), Forschungszentrum Jülich, Lichtenbergstr. 1, 85747 Garching, Germany

<sup>2</sup>Institut für Chemie, Technische Universität Berlin, Berlin, Germany

<sup>3</sup>Jülich Centre for Neutron Science (JCNS) and Institute for Complex Systems, Forschungszentrum Jülich, D-52425 Jülich, Germany,

E-mail: o.holderer@fz-juelich.de

**Abstract.** Grazing Incidence Neutron Spin Echo Spectroscopy (GINSES) opens new possibilities for observing the thermally driven dynamics of macromolecules close to a rigid interface. The information about the dynamics can be retrieved as a function of scattering depth of the evanescent neutron wave, on the length scale in the range of some 10-100 nm. Using a classical neutron spin echo spectrometer with a laterally collimated beam, dynamics can be measured in grazing incidence geometry. We show examples of how the interface modifies the dynamics of microemulsions, membranes and microgels. Instrumental details and possible improvements for this technique will be presented. The key issue is the low intensity for dynamics measurements with an evanescent neutron wave. Conceptual questions how a specialised instrument could improve the experimental technique will be discussed.

## 1. Introduction

Small angle neutron scattering under grazing incidence conditions (GISANS) allows to study structural features close to a rigid interface [1][2]. The neutron beam is directed to an interface between typically a silicon block and the sample below the critical angle. An evanescent neutron wave is then travelling parallel to the surface with a penetration depth of 10 - 100 nm perpendicular to the surface. The scattered neutrons from the evanescent wave are recorded to get structural information lateral and perpendicular to the rigid interface on a nanometer length scale. Recently, this technique has been also applied to study the dynamics of mesoscopic objects close to the rigid interface [4][5][8] with Neutron Spin Echo (NSE) spectroscopy. NSE spectroscopy has the highest energy resolution of all spectroscopic techniques [6][7] in neutron scattering and allows to study the dynamics of macromolecules such as thermal fluctuations of surfactant membranes [9][10] or internal motion of proteins [3]. NSE spectroscopy under grazing incidence conditions (GINSES) is sensitive to thermal fluctuations close to the interface and by varying the penetration depth of the evanescent wave the dynamics as a function of distance to the interface can be measured. The penetration depth is of the order of 10-100 nm. Figure 1 shows a bicontinuous microemulsion measured in GISANS geometry. The interface imposes a lamellar phase for the first membrane layers, giving rise to a Bragg peak in the detector image, while the bulk microemulsion at larger distances to the interface contributes with a



Debye-Scherrer like scattering contribution [4]. The typical  $Q$ -value for a GINSES experiments is indicated with the red circle in the GISANS plot (on the  $Q_y=0$  axis). The large sample cell and the slit geometry of the beam results in a poor resolution for  $Q_y \neq 0$ , all measurements so far were restricted to the  $Q_y=0$  axis. Sensitivity for fluctuations perpendicular to the interface is obtained, e.g. the membrane fluctuations of microemulsions.

## 2. GINSES at an existing (standard) NSE spectrometer

A series of experiments under grazing incidence has been carried out at the J-NSE spectrometer at the FRM II [7]. An entrance aperture in front of the first precession coil has limited the beam laterally to a width of 2 mm, the sample aperture has been adapted to the footprint of the sample cell (also about 2 mm). The sample cell consists of a silicon block (1 or 2 cm thick) where the beam enters at the front side and is then totally reflected at the inner surface to the sample. Different types of sample cells have been used (from GISANS or reflectometry experiments) with a length of 8 or 15 cm. The sample cell can be temperature controlled with a water thermostat. The scattered beam passes through the silicon block and follows then the standard flight path of the NSE spectrometer to the detector. The only difference to a standard experiment is therefore the use of the strong lateral collimation with slit apertures and the appropriate sample cell. The collimation and the small sample volume illuminated with the evanescent wave leads to an intensity loss of the order of  $1/10^4$ . A very high instrumental stability (stable currents, no thermal effects at the coils) and a low magnetic and radiation background of the surrounding is mandatory for such GINSES experiments.

The GINSES technique has been applied to microemulsions [4][5][12] and microgels [11] near interfaces. As an example, the dynamics of a lamellar microemulsion, consisting of  $d$ -decane and  $D_2O$  to equal amounts, and 32% of the surfactant  $C_{10}E_{44}$ , and the influence of the scattering vector is presented (Figure 2). Due to the low scattering intensity in most experiments the whole 2D-detector has been evaluated to capture the largest possible solid angle. When the statistics is good enough, the detector can be divided into regions of different  $Q$ . Here, three  $Q$ -values have been extracted from measurements on lamellar microemulsions by dividing the 2D detector into three slices of different  $Q$ . Besides the lamellar phase in GISANS geometry, also a bulk lamellar has been measured for comparison. The sample is placed in a cell made especially for lamellar microemulsions, having 60 quartz plates over the 30 mm sample width. The microemulsion orients along the quartz plates with the normal of the planes parallel to  $Q$ . The SANS data (top left in Figure 2) showed distinct peaks of the lamellar ordering. NSE measurements with the center of the detector set to  $Q=1.1 \text{ nm}^{-1}$  have been performed just in front of the second peak. The relaxation time in such microemulsions typically slows down significantly at the position of the correlation peaks, with  $1/\tau \propto 1/S(Q)$  (often referred to as “de Gennes narrowing”). The slowing down of the dynamics when approaching the correlation peak at  $Q=1.5 \text{ nm}^{-1}$  with the relaxation time increasing from  $\sim 140 \text{ ns}$  for  $Q=1.0 \text{ nm}^{-1}$  to  $180 \text{ ns}$  for  $Q=1.3 \text{ nm}^{-1}$  (top right in Figure 2) reflects the  $1/\tau \propto 1/S(Q)$  behaviour of the relaxation time. The situation is different for measurements of the same sample under grazing incidence (bottom left and right in Figure 2). There the flat interface is only imposed on one side of the sample, which obviously reduces the range of the ordering. The relaxation time decreases continuously with increasing  $Q$ . The difference in the relaxation time between grazing incidence conditions and incident angles above the critical angle is not significant. The highest  $Q$  has also the fastest dynamics in GINSES-measurements on this sample (in bicontinuous microemulsions a  $Q^3$ -dependence would be expected for  $1/\tau$ [9], here the  $Q$ -range is too limited to quantify the exact  $Q$ -dependence). The difference in absolute relaxation time is also at least partly attributed to the much better ordering of the microemulsion in the lamellar cell.

A second group of experiments focused on the internal dynamics in a thin layer of adsorbed charged microgel particles [11]. Although the intensity is extremely low, the intermediate

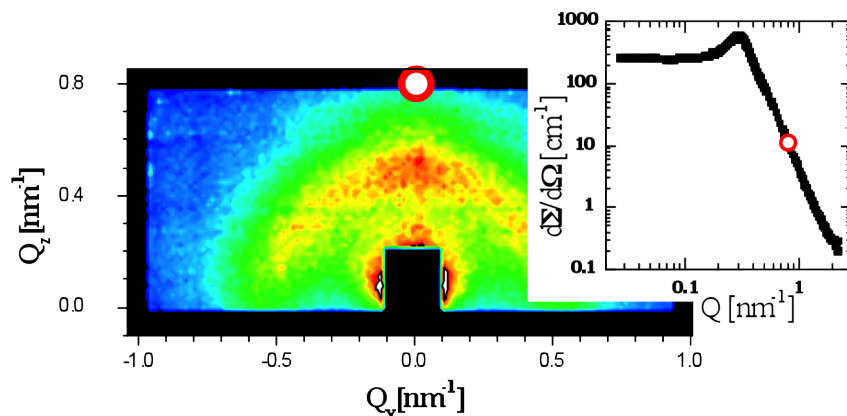


**Figure 1.** GISANS detector image of a bicontinuous microemulsion near a Si interface. It shows a superposition of the peak from the lamellar phase at the interface and the Debye-Scherrer like ring from the bulk microemulsion. The inset shows a scattering curve of a standard SANS experiment of a bicontinuous microemulsion with the characteristic correlation peak. Most GINSES experiments have been carried out at  $Q=0.8 \text{ nm}^{-1}$  as a compromise between probing local dynamics at high  $Q$  and high intensity at low  $Q$ .

scattering function  $S(Q,t)$  could be measured for rather low  $Q$ -values of  $Q=0.6 \text{ nm}^{-1}$ . The dynamics of these particles was strongly dependent on the charge of the microgels. The charge state was tuned by protonation of the carboxylic acid groups in the network. For being in the easily accessible dynamic range, even neutral and slightly charged particles were studied in the first set of experiments. Compared to bulk phase diffusion the dynamics seems to be strongly slowed down in this system. Moreover, first data suggest a depth dependence of the dynamics. More details can be found elsewhere [11].

### 3. New concepts

#### 3.1. Instrument

The flight path after the scattering event has to be undisturbed and the solid angle covered by a 2d-detector of about  $30 \times 30 \text{ cm}^2$  has to be used to gather the maximum possible intensity. The usual setup as for a normal NSE instrument is required, including the correction coils for reducing the field inhomogeneity of the off-axis flight paths in the solenoid. The two precession regions of a spin echo spectrometer (before the scattering event and after the scattering event) have to be symmetrical. Therefore, the magnetic layout of a GINSE instrument must be basically the same as for a standard NSE instrument.

Possible gains can be achieved in front of the precession paths by preparing a beam already in the desired shape (laterally narrow, but high). The flight path of typically 4 m between the end of the neutron guide and the sample in a NSE spectrometer acts as a collimation distance, the lateral divergence of the beam has to be small enough such that the neutrons hit the sample. Fig. 3 shows a possible neutron optics design which improves the intensity at the sample. McStas simulations were made where the beam (initially 30 mm in height and 45 mm in width in this example, the scale on the figure is different for x- and y- direction) is split into 3 pieces, the outer two pieces are then guided on top and below the middle part respectively. In a first section, the outer pieces are directed upwards and downwards respectively, until they are one height of the neutron guide displaced, then the three parts of the beam are reflected by a polarizing mirror into the new direction, each polarizer section displaced by half of the polarizer length. In this way, all parts of the beam are finally on top of each other, with the same divergence as in

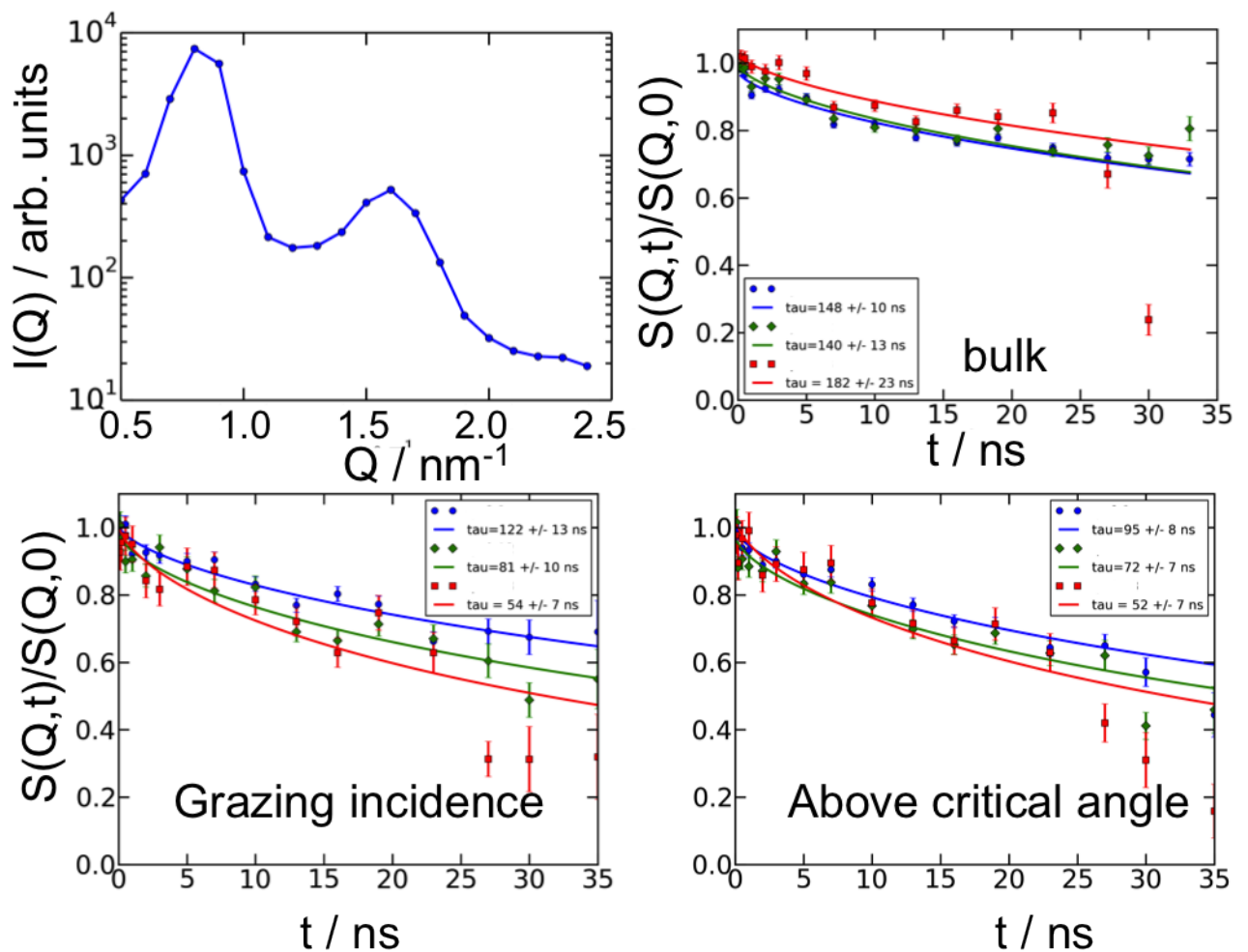


**Figure 2.** Top left: Small angle scattering of a lamellar microemulsion (bulk sample), oriented in a cell with 60 parallel quartz plates. The dynamics at  $Q=1.0 - 1.3 \text{ nm}^{-1}$  shows the slowing down when approaching the next scattering peak (top right; the plots showing  $S(Q,t)$  show always the three  $Q$ -values 1, 1.1,  $1.3 \text{ nm}^{-1}$  in this order). With the GINSES sample cell the slowing down is not observed, neither under grazing incidence conditions, nor above the critical angle (bottom left and right respectively).

the beginning. The ideal gain of such a configuration would be a factor of 3, the first McStas-trials lead to a factor of 2 in gained intensity. The gain has been determined from the McStas simulations with a monitor having the size of the sample footprint (3mm wide, 50mm high) at the sample location (approx. 4 m behind the end of the neutron guide). Only neutrons with a sufficiently small divergence reach therefore the sample monitor. The divergence has been checked with a lambda-divergence monitor, which registers the divergence for the different wavelengths (Fig. 3, right). In front of the beam splitting section and at the end of the neutron guide, the divergence was approximately  $\pm 0.15^\circ$ . This setup requires at least 3 reflections, including one polarizing reflection. A setup for beam shaping with only two reflections might be possible with two inclined mirror planes for each part of the neutron beam.

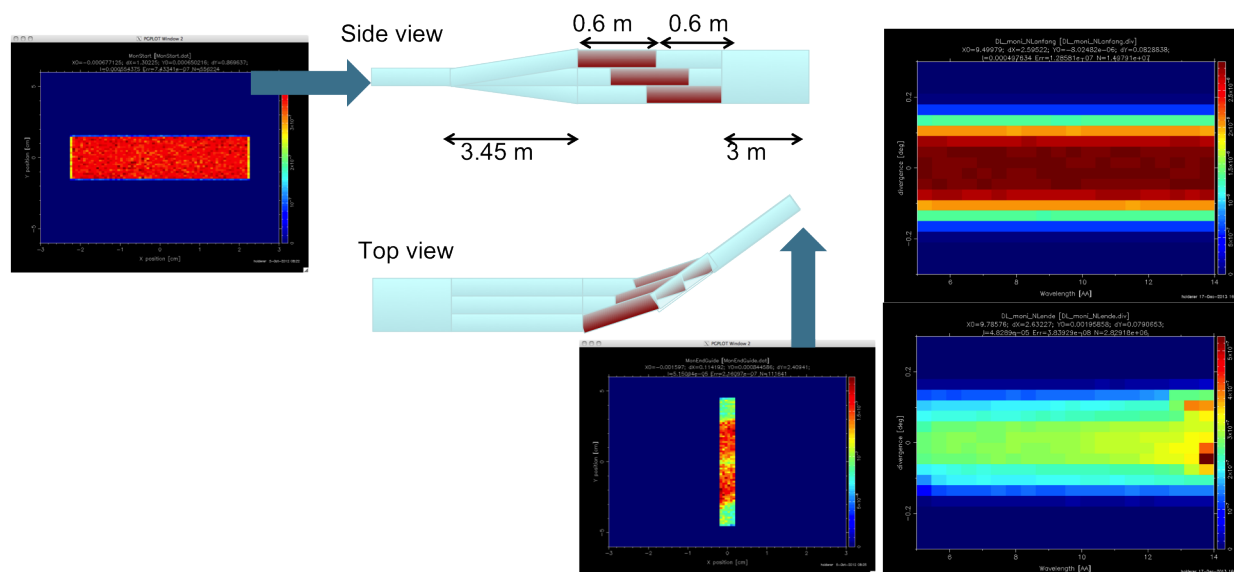


**Figure 3.** right: Possible realization of a neutron guide system with optimized geometry. The divergence is preserved and not increased with this setup, giving the advantage over a simple trumpet- and antitrumped design. left: plots of a neutron divergence monitor: divergence vs wavelength in the range of 5-14 Å, at the beginning of the beam splitter and at the end of the neutron guide system. In both cases the divergence is approximately  $\pm 0.15^\circ$ .

### 3.2. Sample cell and environment

A gain in intensity (possibly by a factor of 2-3) is possible with an optimized cell design. The beam height (which is limited to about 40 mm at the J-NSE spectrometer) could be further increased along with a higher sample cell. The longest cells we have used so far are with 150 mm at the limit, where the transmission of the Si block is still acceptable. A prism in front of the sample cell allows to get a very well defined scattering depth, even for large wavelength bands [12]. Although first tested at a pulsed source at the SNS-NSE for the larger wavelength band available there [13], this option is especially suited also for instruments at continuous sources. The well defined scattering depth for all wavelengths at one setting allows to change the wavelength while staying at the same scattering depth. One can then easily extend the measured timerange with some extra Fourier times at longer wavelengths (a procedure which is commonly used for standard measurements). Secondly, the extreme angles (incident angle of "zero" or the critical angle) can be approached with a much higher precision when the scattering depth is better defined.

An important topic are auxiliary techniques at the sample position. It is desirable to have a quality control of the sample right at the start as well as for the duration of the rather long experiment (typically one to several days for one sample). Different kinds of monitoring and measuring equipment at the sample position can be envisaged. Diffusing wave spectroscopy might be an option for online monitoring of concentrated and turbid samples. One interesting technique in this context is evanescent wave dynamic light scattering (and variations thereof), which can provide dynamic information on larger length- and timescales than GINSEES. Besides the extension of the dynamic range it can also monitor the quality of the sample.

## 4. Conclusion

We presented examples of neutron spin echo investigations near a solid surface with the possibility of varying the penetration of the evanescent wave and hence the probing distance.

Thermal fluctuations of microemulsions and microgel particles in the vicinity of the interface have been investigated, and modifications of the thermal motion by the solid surface could be detected. The low intensity of the technique due to the strong lateral collimation of the beam requires a very stable instrument with a low and constant background. An optimized neutron beam transport and sample environment would allow to increase the intensity at the sample by a factor of about 5 compared to the situation at current NSE instruments which would allow to study a wider class of samples. Auxiliary monitoring and measuring techniques at the sample position like e.g. evanescent wave dynamic light scattering could help to gain additional information simultaneously and to monitor the sample quality throughout the rather long experiment.

- [1] P. Müller-Buschbaum, J.S. Gutmann, R. Cubitt, M. Stamm, *Colloid Polym Sci* **277**, 1193-1199 (1999)
- [2] M. Kerscher, P. Busch, S. Mattauch, H. Frielinghaus, D. Richter, M. Belushkin, G. Gompper, *Phys. Rev. E* **83**, 030401 (2011)
- [3] R. Biehl, B. Hoffmann, M. Monkenbusch, P. Falus, S. Preost, R. Merkel, D. Richter, *Phys. Rev. Lett.* **101**, 138102 (2008)
- [4] H. Frielinghaus, M. Kerscher, O. Holderer, M. Monkenbusch, D. Richter, *Phys. Rev. E* **85**, 041408 (2012);
- [5] H. Frielinghaus, O. Holderer, F. Lipfert, M. Kerscher, S. Mattauch und D. Richter, *EPJ Web of Conferences*, **33**:03005 (2012)
- [6] M. Monkenbusch, R. Schätzler, D. Richter, *Nucl. Instr. and Meth. In Phys. Res. A* **399**, 301 (1997)
- [7] O. Holderer, M. Monkenbusch, R. Schätzler, H. Kleines, W. Westerhausen, D. Richter, *Meas. Sci. Technol.* **19**, 034022 (2008)
- [8] M. Walz, S. Gerth, P. Falus, M. Klimczak, T.H. Metzger, A. Magerl, *J. Phys. Cond. Mat.* **23**, 324102 (2011)
- [9] O. Holderer, H. Frielinghaus, D. Byelov, M. Monkenbusch, J. Allgaier, D. Richter, *J. Chem. Phys.* **122**, 094908 (2005)
- [10] S. Wellert, M. Karg, O. Holderer, A. Richardt, T. Hellweg, *Phys.Chem.Chem.Phys.* **13**, 3092 (2011)
- [11] S. Wellert et al., in preparation
- [12] H. Frielinghaus, O. Holderer, F. Lipfert, M. Monkenbusch, N. Arend, D. Richter, *Nucl. Instr. and Meth. In Phys. Res. A* **686**, 71-74 (2012)
- [13] M. Ohl et al., *Nucl. Instr. and Meth. In Phys. Res. A* **696**, 85 (2012)
- [14] M. A. Plum, S. D. B. Vianna, A. Unger, R. F. Roskamp, H.-J. Butt, B. Menges and W. Steffen, *Soft Matter* **7**, 1501 (2011)
- [15] G. Fytas, S. H. Anastasiadis, R. Seghrouchni, D. Vlassopoulos, J. Li, B. J. Factor, W. Theobald and C. Toprakcioglu, *Science* **274**, 2041 (1996)